Shape deviations of DLW microstructures in dependency of fabrication parameters

OPEN ACCESS
IOP Publishing
Journal of Micromechanics and Microengineering
J. Micromech. Microeng. **31** (2021) 125002 (8pp)
https://doi.org/10.1088/1361-6439/ac2a14

Shape deviations of DLW microstructures in dependency of fabrication parameters

Sven Fritzsche*, Ievgenia Topolniak, Matthias Weise and Heinz Sturm

Bundesanstalt für Materialforschung und -prüfung, Unter den Eichen 87, Berlin, 12205, Germany

E-mail: sven.fritzsche@bam.de

Received 25 May 2021, revised 31 August 2021
Accepted for publication 24 September 2021
Published 14 October 2021

Abstract

Deep understanding of the effects associated with fabrication parameters and their influence on the resulting structures shape is essential for the further development of direct laser writing (DLW). In particular, it is critical for development of reference materials, where structure parameters are precisely fabricated and should be reproduced with use of DLW technology. In this study we investigated the effect of various fabrication and preparation parameters on the structural precision of interest for reference materials. A well-studied photo-curable system, SZ2080 negative photo-resist with 1 wt.% Michler's ketone (Bis) photo-initiator, was investigated in this work. The correlation between applied laser power, laser velocity, fabrication direction on the deviations in the structure shape were observed by means of white light interferometry microscopy. Moreover, influence of slicing and hatching distances as well as prebake time were studied as function of sample shape. Deviations in the structure form between the theoretically expected and the one detected after DLW fabrication were observed in the range up to 15%. The observed shape discrepancies show the essential importance of fine-tuning the fabrication parameter for reference structure production.

Keywords: two photon polymerization, 2PP, direct laser writing, SZ2080, shape deformations

(Some figures may appear in colour only in the online journal)

1. Introduction

Direct laser writing (DLW) is a full 3D fabrication technique, where a photoresist is polymerised by a femtosecond laser via absorbing more than one photon simultaneously by applying tightly-focused femtosecond-pulsed light beam, which is based on two or more photon polymerisation [1]. In the focal spot of the beam the probability of non-linear processes is high enough to excite molecules.

Due to the radical or ionic polymerisation process the material solidifies further in the focal spot. Hybrid inorganic–organic materials such as SZ2080 [2, 3] or Ormocers [4] offer a great stability while exhibiting low to no shrinkage beneficial for a wide range of applications. Among other applications micro optics [5–7], cell scaffolds [8–10] and microfluidics [11, 12] have been described in the literature. Shape deviations or surface variances are a drawback for roughness calibration structures as described by Ströer and Eifler [13, 14]. To improve repeatability and find a way towards producing reliable standard structures one has to be able to predict the expected discrepancies in the shape of the final structure based on the selected fabrication parameters.

The size of the polymerised volume in the focal spot is called voxel and has a certain lateral (XY-direction) and longitudinal (Z) dimension. A certain overlap between these voxels leads to the fabrication of a bulk material. The voxel size in XY

* Author to whom any correspondence should be addressed.

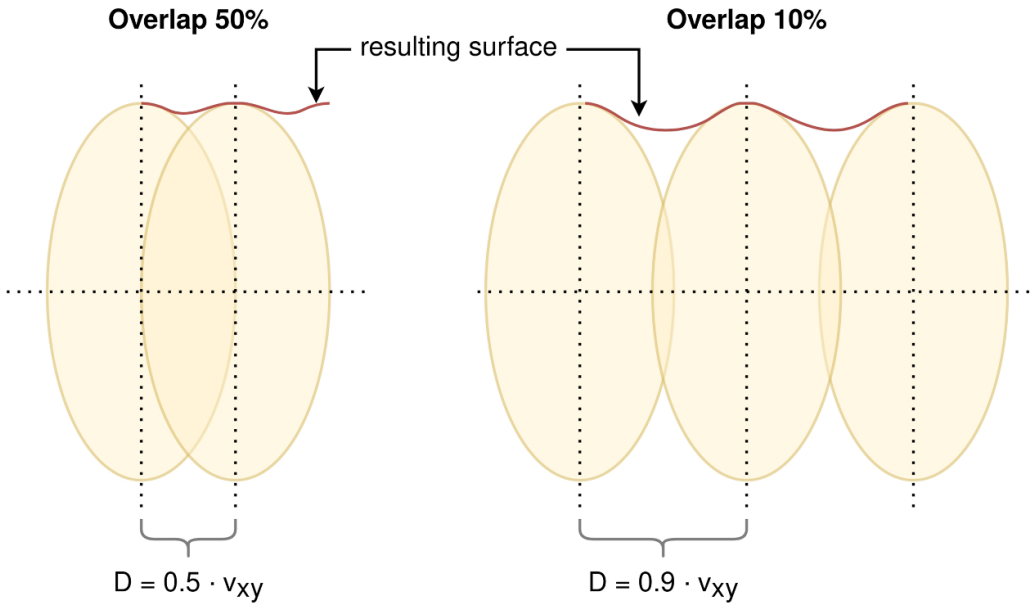

Figure 1. Schematic influence of the overlap shown for 50% and 10% overlap of the individual voxels.

and Z can be quantified from SEM images, when a single line is written between two objects.

Once the obtained voxel sizes for a given fabrication conditions are determined hatching and slicing distances can be calculated with regard to targeted voxel overlap (see equation (1)). Where ε_{xy}, ε_z is the overlap in Percent and v_{xy}, v_z the voxel size in XY- or Z-direction respectively. D is the distance between two voxels, so either the hatching or slicing distance.

$$\varepsilon_{xy} = 1 - \frac{v_{xy}}{D} \cdot 100, \quad \varepsilon_z = 1 - \frac{v_z}{D} \cdot 100. \tag{1}$$

For highly complex shapes such as Triply Periodic Minimal Surfaces [15] or other structures with undercuts a layer-by-layer approach with an automated slicing of the 3D structure by a slicer software is needed. These slicing software are usually provided by the manufacturer of DLW machines. Three-dimensional structures are often available as STL-files and there is a set of basic parameters that can be given to the slicer. These parameters include the distances for hatching—distance between two voxels in XY-plane—and slicing—distance between two slices in fabrication direction—as well as the number of contour lines. Higher hatching distances lead to short production times but a surface with a increased roughness [16]. Nevertheless previously shown by Saha *et al* [17] voxel overlaps as little as 47% can already induce damage to the structure. An increased absorption of single-photons in the cured resin was identified as a trigger. So high distances lead to a rough surface by Jonušauskas, whereas low distances lead to internal damage by Saha. In figure 1 the relation between roughness and overlap is shown.

Similar to other 3D fabrication techniques such as Selective Laser Melting [18] or Fused Deposition Modeling [19, 20], DWL artefacts and defects have to be categorised and their origin has to be identified. These defects can include areas with different crosslinking degrees [21], that can lead to unwanted mechanical or optical properties. As well as unwanted porosity, cracks, shape deviations or/and delamination from the substrate.

We investigate the effect of the overlap strategy on the shape of a structure as well as fabrication direction and prebake time for the hybrid polymer SZ2080 with 1 wt.% Michler's ketone as photoinitiator. This photo-resist combination was previously used for applications like microlenses [22], photonic crystals [23] and scaffolds [24]. Before the SZ2080 photo-resist can be polymerised a drying step is needed, which is also called prebake. As described by Ovsianikov *et al* [3] during drying process of SZ2080 'alcohol, water, and any other solvents present in the film are released from the system and the unstructured material shrinks.' A similar behaviour was shown in [25]. In literature different prebake times and temperature regimes can be found.

To be able to quantify shape deviations a simple cube structure will be analysed. We also tested the influence of the time, which is needed to structure one layer in a layer-by-layer approach as these can be dependend of the used slicing software. A bulge instead on the supposed to be flat structures in fabrication direction in various structures was observed. The influence of fabrication parameters like hatching and slicing distance as well as fabrication direction was examined.

2. Materials and methods

2.1. Materials

A list of the used chemicals can be seen in table 1.

2.2. Sample processing

A drop of SZ2080 was casted on a 170 μm glass slide and subsequently prebaked to obtain a hard gel.

Table 1. List of chemicals and their abbreviations used in this work.

Chemicals	Function	Trivial name/Abbreviation
SZ2080	Photoresist	
4,4′-Bis(N,N-dimethylamino)benzophenone	Photoinitiator	Michlers ketone, Bis
4-Methylpentan-2-one	Developer	Methyl isobutyle ketone, MIBK

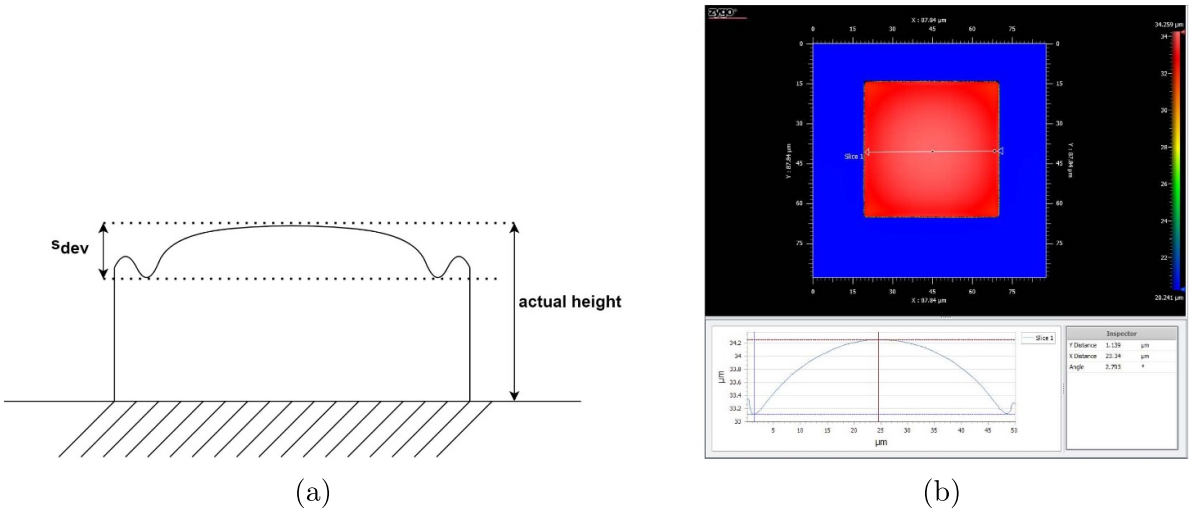

Figure 2. (a) Schematic illustration of structure profile and shape deviation s_{dev} as detected by WLIM and (b) illustrated profiles of the fabricated structures, upper view from the top, bottom: measured profile.

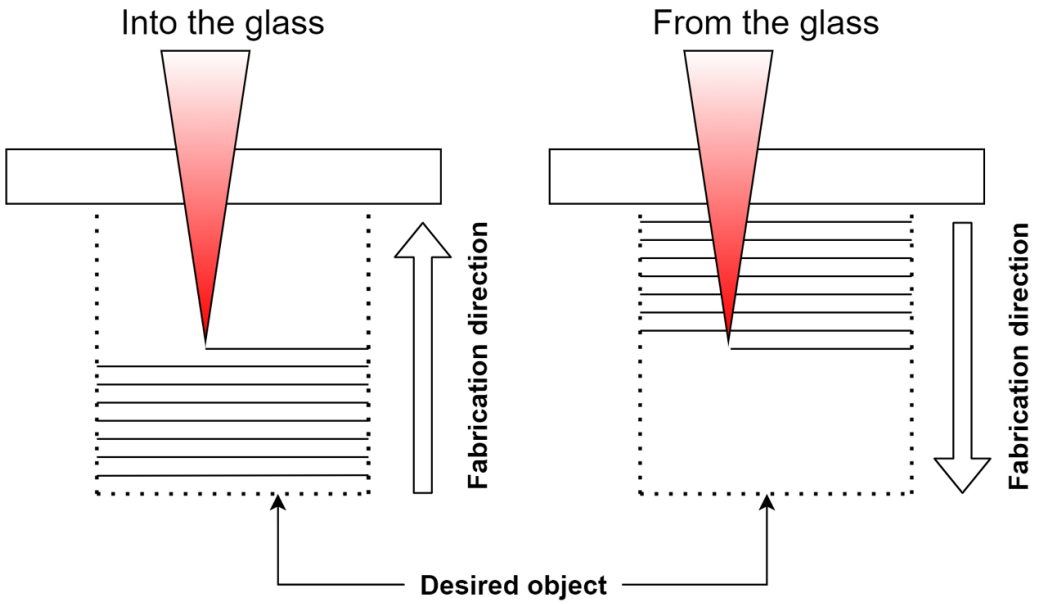

Figure 3. Schematic illustration of fabrication direction 'Into the glass' and 'From the glass', with laser light in red and the already fabricated slices as black line, the dashed line represents the desired object to be fabricated.

A prebake time and temperature of a mandatory 15 min at 50 °C and a following 1 h at 100 °C for all samples unless otherwise specified. The 15 min at 50 °C are used to avoid bubbles in the baked drop, which are trapped gaseous solvents under the already hardened gel surface.

To achieve comparable results all measurements of the same type were done within the same drop/sample. Each fabricated simple cube structure had a side length of 50 μm and a height of 15 μm. Each slice was hatched alternating in X- and Y-direction with one contour line drawn before the hatching

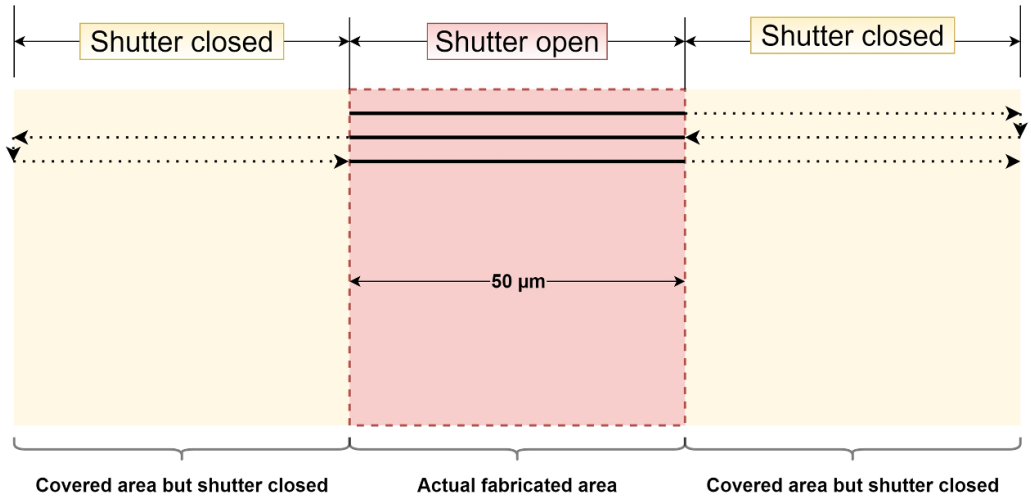

Figure 4. Schematic illustration of fabrication time per layer experiment with the fabricated voxel as solid lines and dashed lines with closed shutter, the red area is the than polymerised area, whereas the yellow area was virtually exposed.

step. After fabrication samples were developed for 45 min in MIBK. All experiments were carried out at a room temperature of 22 °C.

2.3. DLW setup

A Laser Nanofactory from Femtika Ltd (Vilnius, Lithuania) controlled by 3DPoli software (v. 6.33) was used to produce polymer microstructures. The femtosecond light-source was a Erbium-doped fiber laser (C-Fiber High Power from Menlo GmbH, Germany) emitting at 780 nm, 100 fs pulse duration and 100 MHz repetition rate. Plan-Apochromat objective (Carl Zeiss Jena AG) with a magnification of 63× and 1.4 numerical aperture has been used to focus the beam. Laser Nanofactory fabrication was operated by a combined stage/galvoscanner setup meaning that the movement of the X–Y stage (Aerotech) and galvo scanners (Aerotech AGV-10HPO).

2.4. White light interferometry microscopy (WLIM)

With a white light interferometry microscope Ametek-Zygo NewView^{TM} 9000 we measured each structure individually with a 100x Mirau objective with 0.85NA and an optical resolution of 0.34 μm. All samples showed a small overshoot on the edges and which can also be seen in the sematic drawing figure 2(a). The valley thereafter on each edge was than used as baseline from the highest point, the height difference s_{dev} was used to characterise the shape deviation. The height difference s_{dev} was measured along the X-axis. A screenshot of the measured surface in the Zygo mx-software is given in figure 2(b). The value of the shape deviation ρ_{dev} is given as percentage of the given structure height of 15 μm as calculated in equation (2).

$$\rho_{dev} = \frac{s_{dev}}{15\ \mu\text{m}}. \tag{2}$$

2.5. Laser power and velocity

Each polymer-photoinitiator formulation has a specific fabrication window that depends on a range of parameters including those parameters of the fabrication unit (i.e. laser characteristics, optics, polarisation) and the chemical composition of its components and amount of photoinitiator. The production window of used described DLW setup-photoresist combination was determined with an array of power (X-axis) and velocity (Y-axis). The power ranged from 1 to 10 mW and the laser velocity was between 5 and 10 mm s^{-1}.

2.6. Fabrication direction

The structures fabricated in this study were written in either one of the following ways. An illustration is given in figure 3.

- From the glass—first voxel is drawn into the glass and than the rest is drawn through the already polymerised layers of the structure
- Into the glass—first layer is drawn at the top of the object and than the last line is drawn in the glass, object is than attached to the glass

To ensure a connection between structure and substrate at least one layer has to be written in the glass.

2.7. Fabrication time per layer

Most slicing software does not use full freedom of movement of the DLW and instead applies a layer-by-layer approach to cut the desired structure in slices. One can simulate a bigger fabrication area for a slice and the influence this additional time has on the resulting shape that is needed to fully polymerise one layer. On each side of our structure we added the another area to be polymerised but here the shutter was closed. Thus we called this experiment 'Virtual fabrication time' as the virtual fabricated area increases, whereas the actual structured area stayed the same. The principle is shown in figure 4. The

experiment was designed in such a way that total fabrication time increases but the time needed to structure one layer of a structure with a side length of 50 μm stays the same. The virtual scanned area was between 1x and 8x the actual size of the structure. Hatching and slicing distances were 200 and 400 nm, respectively.

3. Results

3.1. Fabrication window

As it can be seen in figure 5 below a power of 2 mW no structures were observed. Structures with 3 and 4 mW showed significant structural defects due to underpolymerisation.

To ensure a minimal amount of shrinkage as described in [26] and a reasonably short fabrication time a laser power of 6 mW and a velocity of 8 mm s^{-1} was selected for further fabrication procedures. For this power-velocity combination the voxel size was determined with 396 nm ($\pm$36 nm) in and 880 nm ($\pm$15 nm) in lateral (XY-) and longitudinal (Z-direction).

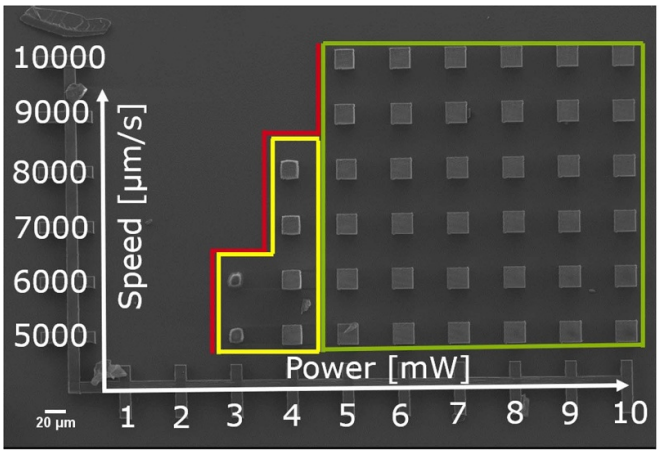

Figure 5. SEM micrograph of the power-velocity array for SZ2080 with 1% bis PI.

3.2. Influence of prebake time and voxel overlap

To investigate the effect of hatching (H) and slicing (S) the structure array within the range of different H and S overlaps was fabricated. For this experiment, a prebake time of 1 h and a printing direction into the glass was applied. The SEM micrograph of resulted array can be seen in figure 6.

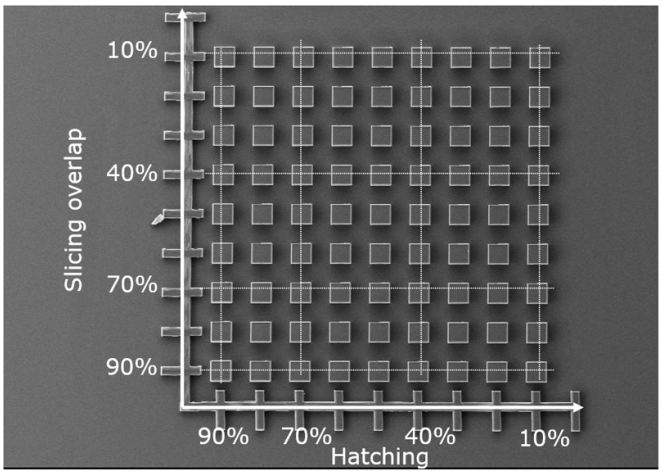

Figure 6. SEM micrograph of SZ2080 structure array fabricated with different slicing and Hatching overlaps. Pre-baking time was 1 h and a fabrication direction 'into the glass' was applied.

For slicing overlaps of 90%, 70%, 40% and 10% we measured the shape deviation ρ_{dev} along the X-axis as described. An influence on the overall results by changing the measuring axis was not observed. One such an array can be seen in figure 6. As shown in figure 7 within the given microstructure array the maximal shape deviation was 10% of the expected size. The increase of the overlap values lead to a decrease of this deviation down to the value of 1.8%. However, for the structures that were produced from the glass substrate into the material bulk, the observed shape deviations were generally lower and were ranged between 3.3% and 1.1% for high and low overlap values, respectively.

Next, we evaluated the structures fabricated 'into the glass' after 3 h of prebake. One could observe ρ_{dev} in the range of 5.3% and 0.55% for high and low overlaps, respectively. For the reversed printing direction this range was between 3% and 1% of the shape deviation respectively. Comparing the experiments in figure 7 with prebake times of 1 and 3 h it is shown that the shape deviations are generally higher for the printing direction 'into the glass' for a prebake time of 1 h. For the printing direction 'from the glass' this was only the case for high overlaps. A visual representation for the measured deviations is shown in figure 8, where high and low shape deviations for an array with 1 h prebake time 'from the glass' are shown.

3.3. Fabrication time

The fabrication time of a structure depends on the laser velocity of the laser as well as on the total length the focal spot has to be moved to fully write the structure. If the hatching distance is doubled a layer will be written in half the time. If the number of slices increases, the fabrication time will increase by the sum of time needed for every additional layer to be printed. In our experiment the smallest hatching and slicing distance was 9x smaller than the highest, therefore the printing time was more than 81 times longer compared to the structure with highest distances.

3.4. Discussion

Structures produced with the fabrication direction 'from the glass' showed significantly lower shape deviations. As each voxel is written into already polymerised volume there is only one direction for the layer to expand or move in Z-direction. Whereas for 'into the glass' the first layer is written freely into the resist and thus the written layer has more freedom to deform within the limits of viscosity of the hardened gel itself. The fabrication direction 'from the glass' may not be usable for all structures due to shadowing. The laser light has

Figure 7. Heatmap with an overview of the experiments on the influence of hatching and slicing overlaps on the shape deviation (value given inside of each tile) for different prebake times and fabrication directions.

to pass through the already polymerised volume and is partially absorbed in it. A similar effect happens when the light is refracted at multiple transitions from gel to polymerised material. It is expected that SZ2080 with higher prebake times had a higher viscosity due to extended drying and hardening effects. Thus the polymerised material has less freedom for movement and deformation. However also the polymerisation itself is inhibited due to a lower diffusion. A similar observed has been previously described for multi-photon absorption by Zandrini *et al* [27] for different monomers and viscosities. It

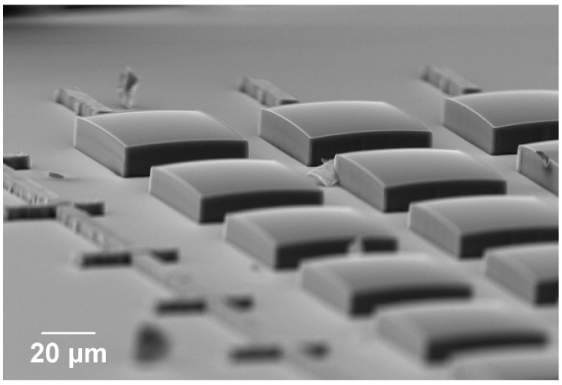

(a) High shape deviations in Z direction

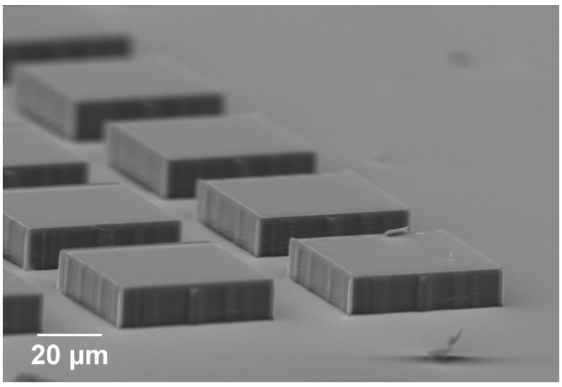

(b) Low shape deviations in Z direction

Figure 8. SEM images of structures with (a) high deviations with 90% overlap in hatching and slicing in the upper left and (b) low deviations with 10% overlap in hatching and slicing for for the structure in lower left, pre-bake time of 1 h and fabrication direction 'into the glass'.

was shown by Zakharina *et al* [28] that Dimethacrylate Ester-Based Compositions at the highest viscosity chain terminations and diffusion propagation happen at lower rate. In [29] it was shown that with an increasing temperature the fabricated SZ2080 the height and diameter of the fabricated pillars also increased. A temperature increase due to high overlaps would also increase temperature in the structure with a resulting expansion of the polymer as in our case. The study by Prielaidas however was conducted with four-beam interference lithography.

The increased deviation of the studied structures with decreased slicing and hatching distances could be explained by the presence heat accumulation. In addition one-photo absorption appears in the already polymerised material as each already written voxel is irradiated multiple times. With lower hatching or slicing distances this effect is intensified. It is possible to count how often an area is above the threshold to start polymerisation. One could image in a slice through the fabricated structure in longitudinal direction. For a slicing and hatching overlap of 90% the maximum amount of times the resist is partially exposed above the threshold for over 81 times. For an overlap of 10% the threshold of polymerisation is in maximum exceeded two times. One time with another voxel in Z-direction and one time with the neighbouring voxel in either direction in X/Y-direction. A model for thermal damage due to the proximity effect was presented by Saha *et al* here [17]. The described damage is based on boiling photoresist. Whereas no structure in this work showed signs of damage, which shows the fabrication below the damage threshold. The observed deformations had multiple causes as outlined earlier.

3.5. *Influence of fabrication time per layer*

If the virtual area was increased from the the actual fabricated 50×50 μm to 8x the size the shape deviation increased by 2% for 'from the glass'-direction and by 3% increase for the 'into the glass'-fabrication direction, which is shown in figure 9. The effect of the time needed to finish one layer and proceed with the next layer is marginal compared to the influence of

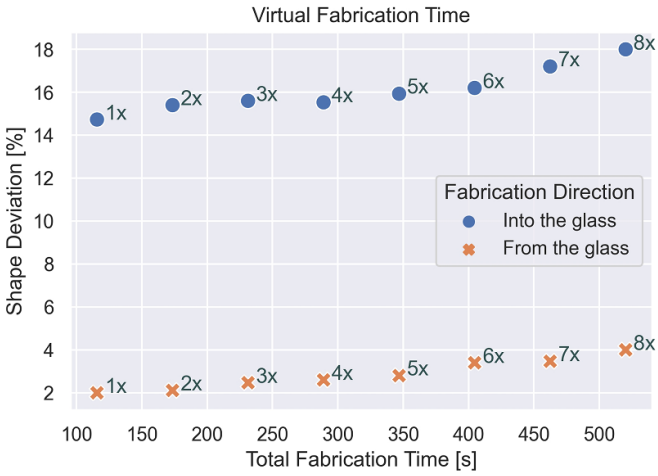

Figure 9. Influence of fabrication time per layer and fabrication direction on shape deviation for multiples of the actual fabricated area.

the fabrication direction. However for large structure it should still be considered to split models in different parts and finish one part after another to keep shape distortions small.

We assume that the shape deviations that occur in the additional time given for each layer between the slices stem from a physical movement. The polymerised layer floats down in the hardened gel due to its mass compared to the unpolymerised surrounding gel. Additional experiments have to be conducted to prove this theory and investigate the influence of gravity as well as prebake time and influences from slicing strategy.

4. Conclusion

Fabrication of the polymer microstructures using DLW technique results in different secondary processes inside of the material that lead to structure distortion, in particular shape expansion. In the current work we show that the hatching and slicing distances have a significant influence on the resulting shape on fabricated objects. Shape deviations as high as

15% (1.5 μm) of the structural shape were observed. With increase of distances, the shape deviation decreases. However, the surface roughness increases with higher hatching distances. Even with very low hatching and slicing distances no boiling of the photoresist was observed. This phenomenon is especially critical when the production of high precision reference materials is targeted. The shape deviations in this study show that fabrication parameters have to be adjusted towards the the used polymer for a reference material. Therefore, the mechanisms of this effect have to be understood and a strategy for its elimination should be defined before mass production.

Also slicing strategies should not be examined individually but always in context with the used photoresist. For a high throughput while maintaining a smooth surface with low deviations one could think about writing the bulk material with low overlaps and high overlaps in the contours. As shown in this work, this effect can be observed although the optimal laser velocity and power as well as hatching and slicing were applied. Shape distortions can not be avoided even under best conditions but minimized by optimizing the parameters.

Data availability statement

The data that support the findings of this study are available upon reasonable request from the authors.

ORCID iD

Sven Fritzsche https://orcid.org/0000-0002-2521-9266

References

[1] Li L and Fourkas J T 2007 *Mater. Today* **10** 30–37
[2] Farsari M, Vamvakaki M and Chichkov B N 2010 *J. Opt.* **12** 124001
[3] Ovsianikov A *et al* 2008 *ACS Nano* **2** 2257–62
[4] Haas K H and Wolter H 1999 *Curr. Opin. Solid State Mater. Sci.* **4** 571–80
[5] Malinauskas M, Gilbergs H, Žukauskas A, Purlys V, Paipulas D and Gadonas R 2010 *J. Opt.* **12** 035204
[6] Guo R, Xiao S, Zhai X, Li J, Xia A and Huang W 2006 *Opt. Express* **14** 810–16
[7] Gissibl T, Thiele S, Herkommer A and Giessen H 2016 *Nat. Photon.* **10** 554–60
[8] Mačiulaitis J *et al* 2015 *Biofabrication* **7** 015015
[9] Ovsianikov A, Schlie S, Ngezahayo A, Haverich A and Chichkov B N 2007 *J. Tissue Eng. Regen. Medicine* **1** 443–9
[10] Weiß T, Hildebrand G, Schade R and Liefeith K 2009 *Eng. Life Sci.* **9** 384–90
[11] Vanderpoorten O, Peter Q, Challa P K, Keyser U F, Baumberg J, Kaminski C F and Knowles T P 2019 *Microsyst. Nanoeng.* **5** 1–9
[12] Jonušauskas L, Rekštyte S, Buividas R, Butkus S, Gadonas R, Juodkazis S and Malinauskas M 2017 *Opt. Eng.* **56** 094108
[13] Ströer F, Hering J, Eifler M, Raid I, von Freymann G and Seewig J 2017 *Addit. Manuf.* **18** 22–30
[14] Eifler M, Hering J, von Freymann G and Seewig J 2018 *Surf. Topogr.: Metrol. Prop.* **6** 024010
[15] Maskery I, Sturm L, Aremu A, Panesar A, Williams C, Tuck C, Wildman R D, Ashcroft I and Hague R J 2018 *Polymer* **152** 62–71
[16] Jonušauskas L, Gailevičius D, Mikoliūnaitė L, Sakalauskas D, Šakirzanovas S and Malinauskas M 2017 *Materials* **10** 12
[17] Saha S K, Divin C, Cuadra J A and Panas R M 2017 *J. Micro and Nano-Manuf.* **5** 031002
[18] Zhang B, Li Y and Bai Q 2017 *Chin. J. Mech. Eng.* **30** 515–27
[19] Uddin M, Sidek M, Faizal M, Ghomashchi R and Pramanik A 2017 *J. Manuf. Sci. Eng.* **139** 081018
[20] Baumann F and Roller D 2016 *MATEC Web Conf.* **59** 06003
[21] Jiang L J, Zhou Y S, Xiong W, Gao Y, Huang X, Jiang L, Baldacchini T, Silvain J F and Lu Y F 2014 *Opt. Lett.* **39** 3034–7
[22] Stankevičius E, Malinauskas M and Račiukaitis G 2011 *Phys. Proc.* **12** 82–88
[23] Tian Y, Kwon H, Shin Y C and King G B 2014 *J. Micro and Nano-Manuf.* **2** 034501
[24] Koroleva A, Deiwick A, Nguyen A, Schlie-Wolter S, Narayan R, Timashev P, Popov V, Bagratashvili V and Chichkov B 2015 *PLoS One* **10** e0118164
[25] Oubaha M, Smaïhi M, Etienne P, Coudray P and Moreau Y 2003 *J. Non-Cryst. Solids* **318** 305–13
[26] Ovsianikov A, Shizhou X, Farsari M, Vamvakaki M, Fotakis C and Chichkov B N 2009 *Opt. Express* **17** 2143–8
[27] Zandrini T, Liaros N, Jiang L, Lu Y, Fourkas J, Osellame R and Baldacchini T 2019 *Opt. Mater. Express* **9** 2601–16
[28] Zakharina M Y, Fedoseev V, Chechet Y V, Chesnokov S and Shaplov A 2017 *Polym. Sci.* B **59** 665–73
[29] Prielaidas Ž, Juodkazis S and Stankevičius E 2020 *Phys. Chem. Chem. Phys.* **22** 5038–45